ResearchGate

See discussions, stats, and author profiles for this publication at: https://www.researchgate.net/publication/295744914

# Bridge vibration and controls: New research

**Book** · January 2012

CITATIONS
33

READS
4,551

**3 authors**, including:

José M Goicolea
Technical University of Madrid / UPM Universidad Politécnica de Madrid
**134** PUBLICATIONS **1,393** CITATIONS

SEE PROFILE

All content following this page was uploaded by José M Goicolea on 26 October 2019.

The user has requested enhancement of the downloaded file.

In: *Bridge Vibration and Controls: New Research* ISBN: 978-1-62100-868-2
Editors: H. Xia, G. De Roeck, J.M. Goicolea ©2012 Nova Science Publishers, Inc.

chapter 3, pp 89-111

***Chapter 3***

# Dynamics of high-speed railway bridges: methods and design issues

***José M. Goicolea, Felipe Gabaldón***
School of Civil Engineering (Escuela de Ingenieros de Caminos), Technical University of Madrid, 28040 Madrid, Spain

## Abstract

In this chapter, a critical review of methods for evaluating dynamic effects on high-speed railway bridges is performed, discussing the features and practical design issues. Closed form solutions for the moving load problem are first discussed and compared to envelopes of impact factors in engineering codes. Moving load models provide the basic tool for dynamic analysis at design stages, with modal analysis or direct time integration. The implications of the number of modes are discussed. The dynamic signature models provide quick methods, which serve to identify critical resonant speeds as well as the agressivity of trains. They serve also as a base for the high-speed dynamic load models. Finally, vehicle-structure dynamic interaction will provide more refined predictions. For general cases, but specially short and medium span bridges, simplified interaction models are advisable. Based on the methods discussed some applications to analysis of design issues are developed. Firstly the influence of the span length of bridges is considered, shorter spans result in more pronounced resonance. An example is shown comparing simply supported and continuous deck bridges, the former are shown to result in significantly higher vibrations. Finally, the influence of variation in the basic mass and stiffness characteristics of bridges is considered, in order to provide simple options to improve design.

## 1 Introduction. Dynamic action of traffic on bridges

Traffic loads on railway bridges are a major action to be considered for guaranteeing safety and functionality of the structures. Not only the traffic loads are larger and more concentrated than for road bridges, but they also produce significant dynamic effects. Furthermore, the nature of the guided traffic on rails imposes more stringent safety requirements than for road vehicles, resulting in limitations to deck accelerations and

deformations. With the advent of faster trains in new high-speed railways the relevance of these dynamic effects has become one of the key design factors for railway bridges.

The dynamic effects on bridges have been since the early days of railways an important concern. The first major accident reported for passing trains in railway bridges was the collapse of the Dee river bridge at Chester in 1847, Lewis (2007). This bridge was designed by Robert Stephenson with cast iron girders, and its collapse caused 5 deaths. Another infamous case is the Tay River Bridge Disaster. The 3.5 km long bridge was built by Sir Thomas Bouch in 1878, its collapse in 1879 left all 75 passengers dead (Lewis et al 2002, Martin et al 2004). From the inquiry which was made at the time, it is interesting to point one of the concluding remarks: "Trains were frequently run through the high girder at much higher speeds than at the rate of 25 mph *(42 km/h)*". There are some discrepancies today as to whether the leading cause for the collapse was the high winds simultaneously to the traffic loads or the fatigue failure enhanced by dynamic effects of traffic loads.

These accidents among other causes motivated the early interest in the study of the dynamic effects of moving loads. The first solutions were proposed by Willis (1849) and Stokes (1849). The classical work by Timoshenko (1928) includes some further developments in dynamic applications to railway bridges. It is interesting to point out the statement in this last work that with the speed of trains at the time the dynamic increment from moving loads on the bridge is evaluated to be under 10%, whereas the greatest risk is deemed to provide from pulsating forces in rotating balance weights of steam engines, with up to 84% increase.

The simplest solution of a moving load on a simply supported bridge involves neglecting the non-suspended mass (wheelsets) as well as the vibrations of the suspended masses, which is a sufficiently approximate solution for many cases. It is easily obtained that the maximum dynamic increment over static effects for this case is $\varphi' = 77\%$, using standard notation for railway structures engineering. This increase is significant, however it may be easily bounded by a dynamic factor in the design codes, which increases the static load effects, the so-called *impact factor*. This has been the basis of the approach followed in engineering codes up to very recently (UIC, 1979), until high-speed trains have arrived.

Figure 1 shows an example for a 15 m simply supported beam-type bridge, for which the computed dynamic increment at 220 km/h, with 2% damping, is $\varphi' = 59\%$. The critical velocity, for the maximum dynamic increment cited above, would be in this case 333 km/h. In real bridges, additional dynamic effects must be considered from the irregularities of tracks and wheels ($\varphi''$ in UIC standard railway structures engineering notation, UIC (1979). However, these are generally of less importance for the bridges (in this case they would amount up to an additional $0.5\varphi'' = 2\%$ dynamic increment for well maintained track, UIC (1979)).

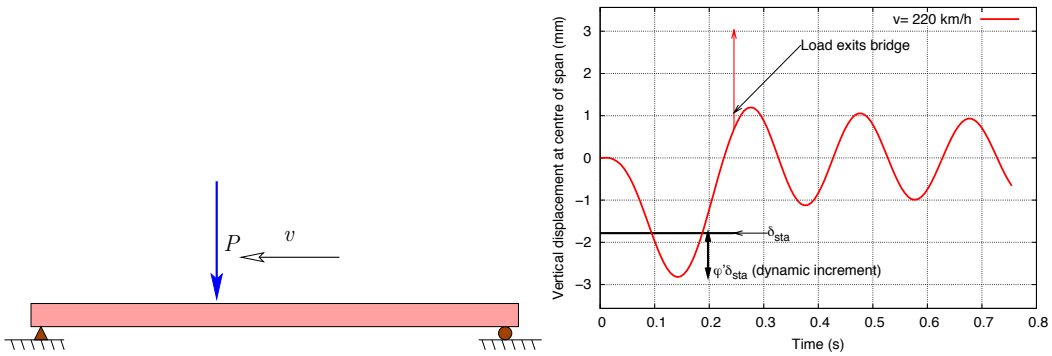


Figure 1. Dynamic increment for moving load on simply supported $L = 15$ m bridge, from catalog of ERRI D214 (ERRI, 1998), with $v = 220$ km/h and damping $\zeta = 0.02$.

The new high-speed trains introduce a potentially much greater dynamic effect, resonance from regularly spaced axle loads at speeds whose effective frequency may coincide with the fundamental frequencies of bridges. As an example, figure 2 shows measured results for a bridge in the Madrid-Sevilla line, from an AVE S100 (ALSTHOM) train at 220 km/h. The bridge is composed of a sequence of simply supported spans with $L = 38$ m. The measured and computed results show an impact coefficient of approximately $(1 + \varphi') = 2.0$, measured with respect to the highest static effects due to the locomotive. This effect would have been even greater for a double unit train (approx. 400 m length). However, this dynamic effect is not so much a problem for the Ultimate Limit State (ULS) of the bridge, as it is sufficiently covered by the safety margins embedded in the normative static vertical load envelope LM71 and the impact coefficient $\Phi$ employed for the design ENV1991-3, CEN, 1995) . However, in this case the functionality of the bridge was impaired: vibrations induced in the catenary posts proved to be excessive and they had to be relocated in new positions. In other cases the resonant dynamic effects may be even of much greater magnitude, and must be therefore avoided in the design of bridges. Resonance is not adequately covered by an impact coefficient and requires a dynamic analysis of the bridge.

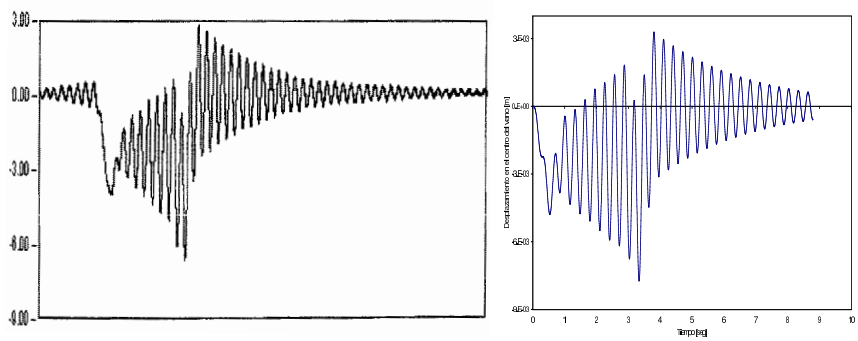

Figure 2. Measured vertical displacement at center of simply-supported span in viaduct over Tajo river, Madrid-Sevilla high-speed line, together with results of simulation with moving load model. AVE S-100 single unit train at 220 km/h

As a result of research carried out in Europe to investigate high speed traffic actions (ERRI, 1998) the new codes for design of railway bridges take into account resonant phenomena from traffic (Eurocode EN1991-2, CEN (2003); leaflet f776-

1, UIC (2006); Spanish code IAPF, Ministerio de Fomento (2007)). In addition to conservative static load models (LM71) and impact factor envelopes $(\Phi)$ they prescribe dynamic analyses to check resonance under certain circumstances. Furthermore they define a High Speed Load Model *HSLM* which provides a dynamic envelope for all European high-speed trains and enables interoperability within the trans-European network (TSI, Technical Specification for Interoperability, ERA (2005)).

In general, it is improbable that the structural ULS would be reached from dynamic traffic actions in bridges designed according to modern standards. More often, the critical issues are Service Limit States (SLS) (Nasarre, 2009) such as the limit of vertical accelerations of the bridge deck. The maximum accepted acceleration of the deck with ballast track is $a_{\max} = 3.5\ \mathrm{m/s^2}$ (EN1990-A1, CEN, 2005), in order to avoid risk of destabilization of the ballast and unacceptable safety risks to the railway traffic. High levels of acceleration are generally observed in short span bridges, due to two reasons: the low overall mass of the bridge, and the fact that the resonant action of the axles (bogies) may be more pronounced for span lengths shorter than the vehicles. Further discussion of this topic is contained in section 3.1.

An additional issue is that related to lateral dynamic response of the bridge-vehicle system under traffic, due to self-excitation (hunting movement, alignment irregularities) or dynamic actions (wind, earthquake). These phenomena arise more seldom, but require considerably more complex models for analysis, as discussed in chapters 6 and 7 of this book. As a result of recommendations in studies by ERRI D181 (ERRI, 1995), some basic limits to lateral compliance of bridge spans have been introduced in Eurocode EN1990-A1 (CEN, 2005), establishing a maximum frequency of 1.2 Hz.

In this chapter we address the models and design issues for dynamic analysis of dynamic effects from traffic, performing a critical review of some aspects and analysing their implications for design. In section 2 the different models available are described. In section 3 some practical design issues and applications are discussed. Finally, some concluding remarks are summarized in section 4.

# 2 Methods for Dynamic Analysis

## 2.1 Dynamic response to moving load

### 2.1.1 Solution for single moving load

The solution to a moving load on a simply supported bridge is well established and available in closed form under certain assumptions. However, it is interesting to review for several reasons. Firstly it provides a basis for defining a dynamic factor (or impact factor) to multiply the static response as a method for design. Additionally, the closed form solution helps to identify clearly the characteristics of the dynamic behavior.

From the dynamic equation of vibration of a beam, the solution may be performed with a modal analysis (Timoshenko, 1928), in which we shall take only the fundamental mode of vibration[1] of frequency $f_0 = \omega_0/2\pi$. For a load at constant speed

[1] In section 2.2 we shall consider the implications of taking one or more modes.

$v$ the *wavelength* is defined as $\lambda = v/f_0$. Additionally, for a bridge of span $L$ a non-dimensional parameter $\alpha$ for the load velocity may be defined as:

$$\alpha = \frac{\lambda}{2L} = \frac{v}{2f_0 L} \ . \tag{1}$$

The time function for displacement at the center of the span, in terms of the maximum static response $y_s = PL^3/48EI \approx 2PL^3/\pi^4 EI$ and considering some simplifications valid for small damping ($\zeta \ll 1$) is:

$$y\,(t) = \frac{y_s}{1-\alpha^2}\left[\sin\left(\alpha\omega_0 t\right) - \alpha \mathrm{e}^{-\zeta\omega_0 t}\sin\left(\omega_0 t\right)\right] \ , \tag{2}$$

where the first term within the brackets is due to the excitation of the external load and the second to the bridge free vibration. This function is valid during the time the load is on the bridge, for which the maximum $y_{\mathrm{dyn}}$ in terms of $t$ may be computed[2]. For the most unfavourable case without damping ($\zeta = 0$) it is attained for $\dot{y} = 0 \ \Rightarrow \ \omega_0 t = \frac{2n}{1+\alpha}\pi$, with the result

$$\frac{y_{\mathrm{dyn}}}{y_s} = \frac{1}{1-\alpha^2}\left[\sin\left(\frac{\alpha}{1+\alpha}2\pi\right) - \alpha\,\sin\left(\frac{1}{1+\alpha}2\pi\right)\right] \ . \tag{3}$$

This expression yields an envelope of the dynamic factor with respect to the non-dimensional parameter $\alpha$, plotted in figure 3. This envelope curve shows a maximum response for a critical value of $\alpha_c$ (and associated critical speed, $v_c$):

$$\alpha_c = 0.617 \quad \Rightarrow \quad \left(\frac{y_{\mathrm{dyn}}}{y_s}\right)_{\mathrm{max}} = (1+\varphi'_{\mathrm{dyn}})_{\mathrm{max}} = 1.768. \tag{4}$$

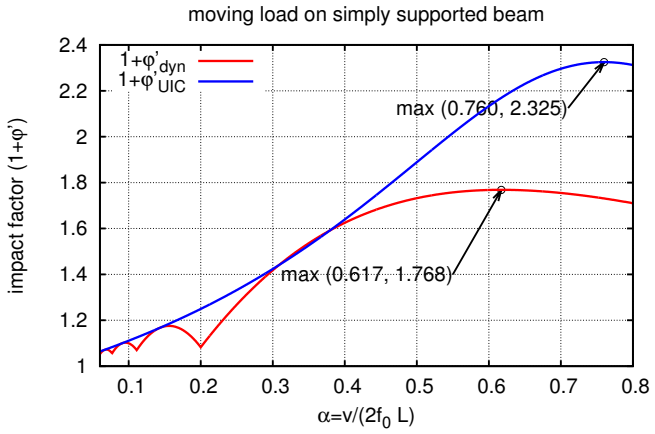


Figure 3: Envelopes of impact coefficient; $\varphi'_{\mathrm{dyn}}$ from analytic solution of moving load, $\varphi'_{\mathrm{UIC}}$ from leaflet f776-1 UIC (1979). The various lobes in the analytic dynamic envelope correspond to the beam performing more than one full oscillation during passage of the load.

As an example, for the bridges in the D214 ERRI catalogue (ERRI, 1998) the maxima of $\varphi'_{\mathrm{dyn}}$ correspond to $v_c = 333$ km/h for $L = 15$ m and $v_c = 356$ km/h for $L = 20$ m, velocities which may be attained by modern high-speed trains.

[2]It may be seen that for the cases of very fast moving loads when the maximum is reached after the load exits the bridge response is lower.

### 2.1.2 Impact factor in engineering codes

The analytical envelope from equation (3) may be compared with the *dynamic factor* for obtaining the dynamic response of *real trains* as defined in UIC f776-1 (UIC, 1979) and Eurocode EN1991-2 Annex C (CEN, 2003)[3]

$$\varphi'_{\mathrm{UIC}} = \frac{\alpha}{1-\alpha+\alpha^4} \ . \tag{5}$$

The dynamic factor to multiply the static response under real trains is then $(1+\varphi'_{\mathrm{UIC}})$. This factor is plotted in figure 3 and compared with the analytical result for dynamic single moving load envelope. It may be observed that it includes a safety margin for speeds corresponding to $\alpha > 0.35$, showing a maximum value of 2.32 (132% increment). The range of validity in the codes for $\varphi'_{\mathrm{UIC}}$ is for conventional rail speeds (i.e. $v \leq 200\ \mathrm{km/h}$).

As a representative example it is useful to apply the evaluation of dynamic effects from the Eurocode EN1991-2 (CEN, 2003), for the above mentioned $L = 15\ \mathrm{m}$ bridge and a train with $v = 200\ \mathrm{km/h}$, which would fall in the conventional speed range. In this case resonance is not considered and the dynamic effects may be evaluated through an *impact factor*. This factor is applied to the static response for the load model LM71 (figure 4)

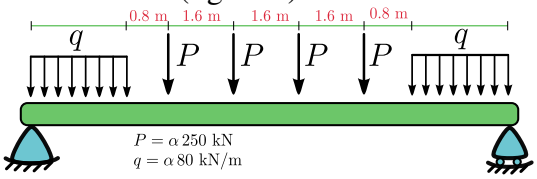


Figure 4: LM71 static vertical load application for simply supported bridge

For carefully maintained track, the dynamic factor applied to static effects of LM71 (EN1991-2, clause 6.4.5.2) is

$$\Phi_2 = \frac{1.44}{\sqrt{L}-0.2} + 0.82 = 1.212 \ . \tag{6}$$

On the other hand, we may evaluate the dynamic factor $\varphi'_{\mathrm{UIC}}$ to be applied for real trains. The value of the non-dimensional velocity is $\alpha = 0.37$, from which

$$(1+\varphi'_{\mathrm{UIC}}+0.5\varphi''_{\mathrm{UIC}}) = 1.5918 \ , \tag{7}$$

where $\varphi'_{\mathrm{UIC}}$ provides from equation (5) and $0.5\varphi''_{\mathrm{UIC}} = 0.0206$ corresponds to additional dynamic effects from track and wheel irregularities, as evaluated defined in UIC f776-1 (UIC, 1979, 2006) and EN1991-2, annex C (CEN, 2003). Considering the proportion between loading of a real passenger train (e.g. consider figure 7) and LM71 (figure 4) is approximately 1/3, results from (7) should be divided y 3 in order to compare with (6). Consequently the envelope dynamic factor $\Phi_2$ is clearly a conservative upper bound for the dynamic effects of real trains at conventional speeds.

For the case of high-speed $(v > 200\ \mathrm{km/h})$ it would be necessary to perform further checks, in particular for maximum accelerations in the deck, and in consequence

[3] In these codes the notation $K$ is employed instead of $\alpha$ in expression (5), with identical meaning.

a dynamic analysis with the methods described below. This particular bridge (single track $L = 15$ m ERRI D214, ERRI (1998)) would not satisfy the criteria set out in table F1 of EN1991-2 and computed accelerations in the dynamic analysis would indeed be excessive, as we shall see in section 2.4.1.

## 2.2 Dynamic analysis with moving loads

The Impact factor, derived from moving load envelopes or analysis of real trains at conventional speeds (i.e. $\leq$ 200 km/h) does not cover resonant effects. These may be of a much greater nature than moving load effects; in order to consider resonance an impact factor approach would be either unsafe or excessively conservative. For circumstances in which there is a possibility of resonance it is necessary to perform a dynamic analysis of the complete train taking into account the complete load sequence (figure 5).

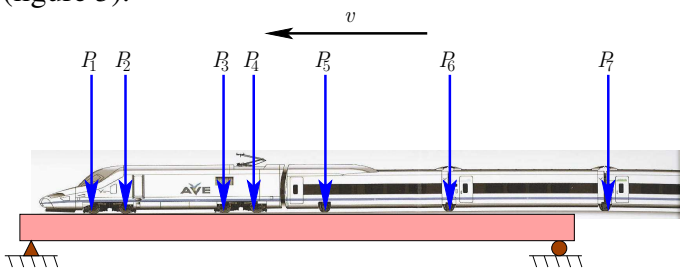


Figure 5: Load sequence from HS train for moving load dynamic analysis

In the simplest case (straight beam subject only to vertical bending) the differential equation that governs the dynamics is

$$\overline{m}\ddot{u}+\left(EI\ u''\right)''=p\left(x,t\right)=\sum_{k=1}^{N}P_k\left\langle\delta(x+d_k-vt)\right\rangle\ , \tag{8}$$

for a train with $N$ concentrated axle loads $P_k$ with offsets $d_k$, where $x$ is the longitudinal coordinate, $u(x)$ the beam vertical displacements, $\overline{m}$ the mass per unit length, and $\delta\left(\cdot\right)$ is the kronecker delta function. The brackets $\langle\cdot\rangle$ have the meaning $\langle\delta(\xi)\rangle=\delta(\xi)$ if $0<\xi<L$ (load within bridge) or 0 otherwise. Superposed dots represent time derivatives and primes $(u')$ derivatives with respect to $x$. This equation may be generalized for arbitrary structures either with 3D beams, torsional effects, shear deformation, or more general continuum-type descriptions. In particular, torsion is added straightforwardly to the above equation. For the sake of simplicity in this work we shall limit our analyses to equation (8).

The solution to equation (8) is obtained in two steps, first in space ($x$ coordinate in this simple case) and then in time. For simple cases the spatial solution can in principle be obtained analytically through modal analysis, obtaining as a result uncoupled modal equations for the amplitude of vibration of each mode (Clough & Penzien, 1993). Considering mode shapes $\phi_i(x)$ and associated circular frequencies $\omega_i$:

$$M_i\ddot{y}_i+2\zeta_i\omega_iM_i\dot{y}_i\ +\omega_i^2M_iy_i=\sum_{k=1}^{N}P_k\left\langle\phi_i\left(x+d_k-vt\right)\right\rangle, \tag{9}$$

where $y_i$ is the modal amplitude for $\phi_i$, $M_i$is the corresponding modal mass and $\zeta_i$ the damping ratio. These equations may be integrated in time by direct numerical algorithms (either coded directly or available within finite element software). As an example, a general code for integration of these modal equations[4] is given in figure 6.

```
for T=h:h:TTL
  for ind=1:length(tren(:,1)) % out=0, in=d_rel
    if ((v*T-tren(ind,3)>L) | (v*T-tren(ind,3) < 0))
       tren(ind,4)=0;
    else
       tren(ind,4)=(v*T-tren(ind,3));
    end
  end
   q  = b;  % d y v para t_n
   q1 = b1;
   P = -((1/(rho*L/2))*peso'*sin(pi*tren(:,4)/L));
   b  = A*q + B*q1 + C*Po + D*P;  % d y v para t_n
   b1 = A1*q + B1*q1 + C1*Po + D1*P;
   b2 = P - 2*zeta*omega*b1 - omega^2*b;
   ii = ii+1;
   res(ii,1) = T; res(ii,2) = b; res(ii,3) = b1;
   res(ii,4) = b2; Po = P; iifin = ii;
end
```

Figure 6: Code for Octave/Matlab for integration of modal equations (9). Coefficients A, B, C, D, A1, B1, C1, D1 as defined in Chopra (2007).

A more general procedure is to employ finite element *(FE)* software for the discretization of the dynamic equations in space. or through the use of finite elements. The only feature which is special for this problem, as regards general structural dynamics problems, is the adequate definition of the actions from the moving loads. As a result of FE discretization the following matrix system of ordinary differential equations is obtained

$$\mathbf{M\ddot{u}} + \mathbf{C\dot{u}} + \mathbf{Ku} = \mathbf{f}\,(t)\ , \tag{10}$$

where $\mathrm{M}$, $\mathrm{C}$ and $\mathrm{K}$ are respectively the mass, damping and stiffness matrices and $\mathbf{f}\,(t)$ the load vector. At this point within FE software it may be chosen to integrate directly in time the coupled equations (10) with a numerical scheme, or to perform a modal analysis of the discretised system and obtain numerical mode shapes and frequencies. These will then be available as uncoupled equations identical to (9) and may be integrated in time individually. The modal analysis option has several advantages. The number of modes to consider can be chosen thus avoiding high-frequency components from higher modes, which are not significant for the bridge response. Moreover, the solution is generally much faster. However, the direct time integration of the complete system provides a more general approach, which may be necessary in some cases, for instance to consider nonlinear effects or contacts.

Following we discuss an application example, solved with a dynamic moving load analysis. It will serve to show some differences with the single moving load solution in section 2.1. In some cases a sequence of two or more axle loads (or bogies) may produce a significant increase from the dynamic effect of a single moving load. In figure 7 we show the case of a representative articulated Electrical Multiple Unit

[4]This algorithm is exact assuming a piecewise linear response, see Chopra (2007)

(*EMU*) at the critical moving load velocity ($\alpha_c = 0.617,\ v_c = 353$ km/h) together with the quasistatic response neglecting inertial vibration. The impact factor produced is $(1+\varphi') = 2.45$, clearly larger than that for a moving load (figure 3). We remark the response in this case is not a case of resonance, but does represent a case for which the simple moving load coefficient is not sufficient, even if it were applied to velocities higher than 200 km/h.

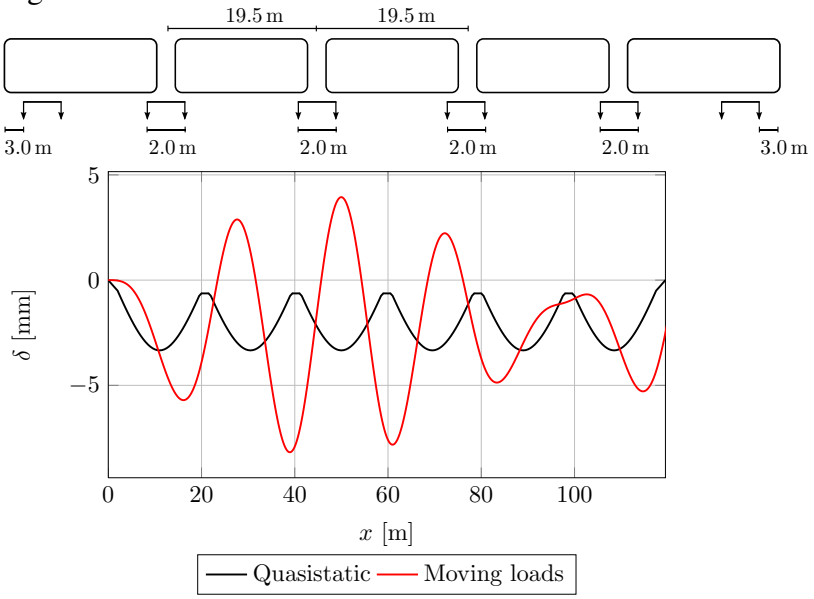


Figure 7: Vertical displacements for $v = 353$ km/h at the center of span of the 20.0 m length bridge of ERRI D 214 catalog (ERRI, 1998) considering moving loads and compared to quasistatic results (no bridge vibrations). Passenger train unit with 5 EMU coaches and articulated bogies, individual axle loads $P = 21.5$ t. The horizontal axis coordinate reflects instead of time the distance $x = vt$ in order to allow appropriate comparison between trains at different speeds.

An issue which may be of importance is the number of modes to consider in the analysis. Generally this decision must be taken based on engineering judgment and a detailed knowledge of the dynamic characteristics of the system. For instance, displacement analysis of a simply supported beam may be generally carried out with only the first (fundamental) mode. Acceleration analysis or the extraction of stresses or sectional resultants will often require more modes to be considered. For acceleration analysis on the bridge it is generally required to consider only frequencies below 30 or 60 Hz, hence higher modes may be directly neglected.

As an example, we present comparative results for the case of the ERRI D214 $L = 30$ m bridge under the ICE3 HS train in figure 8. The fundamental (first symmetric) mode frequency is in this case $f_1 = 3$ Hz, and the second symmetric mode is $f_3 = 27$ Hz (the $2^{nd}$ mode is skew-symmetric and has no influence on mid-span movement). The analysis is performed here for a resonant velocity. It is clear from figure 8 (left) that for displacements only the fundamental mode is significant. However, a significant influence is seen in figure 8 (right) for accelerations from the second symmetric mode. Further modes or even the direct integration with the complete model yields only minor increases to these accelerations.

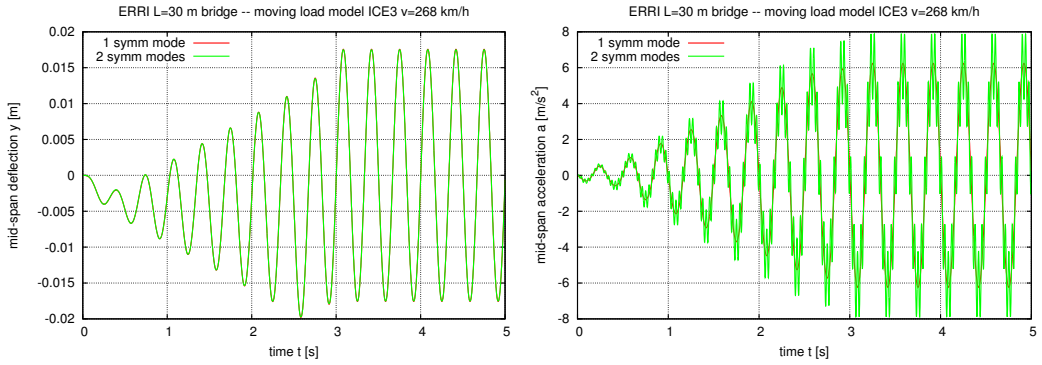


Figure 8: Influence of number of modes for simple bridge, in displacements and accelerations. ICE3 HS train at $v = 268$ km/h on $L = 30$ m bridge from ERRI D214 catalogue (ERRI, 1998)

In order to study the influence of the number of modes for other magnitudes, such as stresses or section resultants, we present as a representative example a basic dynamic analysis that admits a closed form solution. This will not be a moving load but a simply supported beam under a step load $P$ applied at the center. The solution may be developed as the sum of modal contributions. We present as a function of time the shear resultant $Q$ particularized at $x = 0$, that is the reaction load at one support:

$$Q\left(0,t\right) = \frac{-2P}{\pi}\sum_{n=1}^{\infty}\left[\frac{1}{\left(2n-1\right)\left(-1\right)^{n-1}} - \frac{\cos\left(\omega_{2n-1}\sqrt{1-\zeta_{2n-1}^{2}}t\right)}{\left(2n-1\right)\left(-1\right)^{n-1}}\mathrm{e}^{-\zeta_{2n-1}\omega_{2n-1}t} + \right.$$
$$\left. + \frac{\frac{\zeta_{2n-1}}{\sqrt{1-\zeta_{2n-1}^{2}}}\sin\left(\omega_{2n-1}\sqrt{1-\zeta_{2n-1}^{2}}t\right)}{\left(2n-1\right)\left(-1\right)^{n-1}}\mathrm{e}^{-\zeta_{2n-1}\omega_{2n-1}t}\right], \qquad (11)$$

where $\omega_{\mathrm{n}}$ and $\zeta_{\mathrm{n}}$ are respectively the angular frequency and damping ratio for mode $n$. This closed form solution enables an easy comparison of the influence of the number of modes, presented in figure 9, where also the results from a FE analysis with direct integration of the complete model are shown. It is seen that an accurate representation of the shear force needs 10 modes, although for displacement analysis only the fundamental first mode would be sufficient. Further results are available in Goicolea & Gabaldón (2008).

The above remarks may be relevant in practical situations, in which often a dynamic analysis is performed based only on the displacement results. Some problems may require the direct evaluation of dynamic stresses or resultants, in which cases the influence of the number of modes for convergence needs to be properly checked. The resultant dynamic factor may differ to that found for displacements.

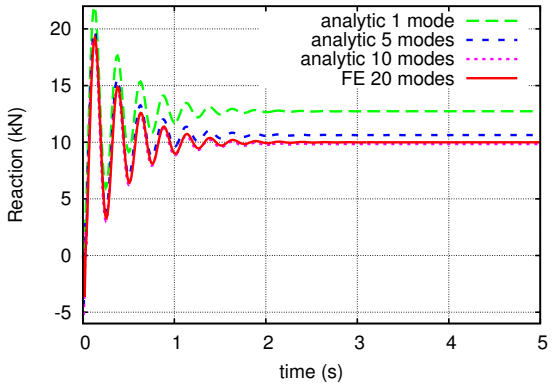


Figure 9: Reaction force at support for simply supported beam under step load for different models

## 2.3 Dynamic signature

As has been said, for simply supported bridges the analysis may be based only on the first fundamental mode, and as a result the overall response consists in a sum of damped harmonics. Each load will result in a damped harmonic term after leaving the bridge (second term within the brackets in equation (2)). If some simplifications are performed, neglecting terms that are not significant for resonant conditions, it is possible to obtain closed form scalar bounds of this series of harmonics. Such is the base of the methods based on the dynamic signature of trains developed in Tartary & Jobert (2000) and ERRI (1998) and included in new codes (EN1991-2, CEN, 2003; IAPF, Ministerio de Fomento, 2007). Two similar but not identical methods are developed in the above references: DER (Decomposition of Excitation at Resonance) and LIR (Residual Influence Line). More details may be found in Domínguez Barbero, 2001. The hypotheses for these methods are:

1. Simply supported bridges under moving loads
2. Only the first (fundamental) mode is considered
3. Some terms are neglected which are small with respect to resonant vibration response

Here we shall employ the LIR model, which considers the residual free vibrations as each axle exits the bridge. The forced terms as the load is on the bridge are neglected, which is a reasonable assumption at resonance. The expressions for the maximum acceleration at the center are:

$$\Gamma = C_{\text{accel}}\, A(\alpha)\; G(\lambda)\;, \quad \text{with } C_{\text{accel}} = 1/M\;,$$

$$A(\alpha) = \frac{\alpha}{1-\alpha^2}\sqrt{\mathrm{e}^{-2\zeta\pi/\alpha} + 1 + 2\cos\left(\frac{\pi}{\alpha}\right)\mathrm{e}^{-\zeta\pi/\alpha}}\;, \tag{12}$$

$$G\left(\lambda\right) = \max_{i=1..N} \sqrt{\left[\sum_{x_1}^{x_i} P_i \cos(2\pi\delta_i) \mathrm{e}^{-2\zeta\pi\delta_i}\right]^2 + \left[\sum_{x_1}^{x_i} P_i \sin(2\pi\delta_i) \mathrm{e}^{-2\zeta\pi\delta_i}\right]^2},$$

where $\delta_i = (x_i - x_1)/\lambda$ are the non-dimensional coordinates of each axle within the train. The result is based on the product of three terms: 1) a constant $C_{\text{accel}}$; 2) a function $A\left(\alpha\right)$ which does not depend on the train and may be interpreted as a *dynamic influence line of the bridge*, depending on its span through parameter $\alpha$; and 3) a function $G\left(\lambda\right)$ which is called the *dynamic signature of the train*, as its shape only depends on the characteristics of the axle load sequence of each particular train. A similar expression may be obtained for displacements by changing the constant factor, see the above references for details.

This model avoids the explicit dynamic analysis requiring only an algebraic evaluation of equations (12). The results may not be strictly an upper bound for non-resonant cases, but they provide a reasonably tight upper bound for resonant cases which are the critical ones.

As an example, in figure 10 the signature of HS train ICE2 is shown for different levels of damping in the bridge. This function shows a resonant peak when the wavelength $\lambda$ equals the length of the coach $L = 26,4\ \mathrm{m}$ and secondary peaks for $L/2$, $L/3$ etc. Signatures for other trains will vary, depending on characteristic lengths between axles and load values.

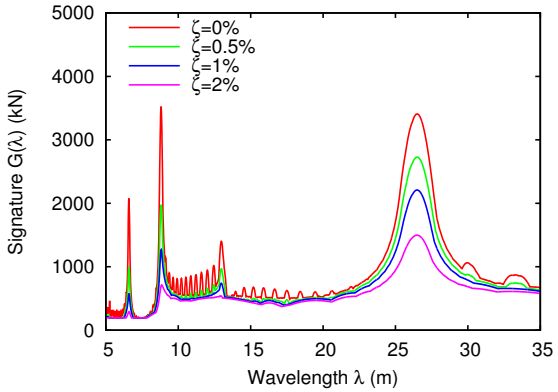


Figure 10: Dynamic signature for ICE2 HS train, for different levels of damping.

A practical application of the signature may be performed to obtain an envelope of maximum accelerations in terms of train velocity. Figure 11 shows the results for ICE2 train and the ERRI D214 bridge $L = 15\ \mathrm{m}$ $(f_0 = 5\ \mathrm{Hz})$, with $\zeta = 2\%$, for speeds between 100 and 400 km/h. It is compared to the results of a similar velocity sweep performed with dynamic analysis of moving loads. As expected, the signature model is an upper bound for the critical range of velocities ($v > 200\ \mathrm{km/h}$). For some velocities, e.g. 175 km/h, the results are not a conservative estimation, however this lacks significance as these values are lower and not critical for design.

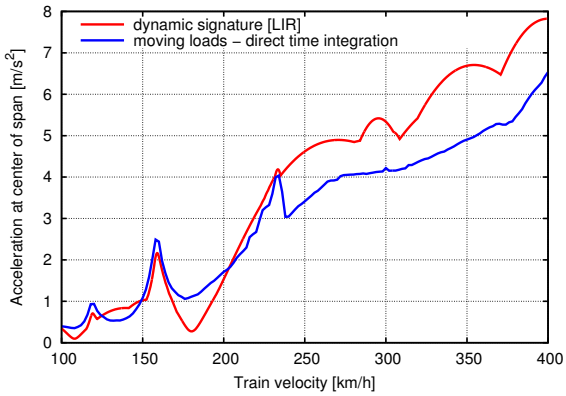


Figure 11: Application example: velocity sweep for maximum accelerations for ICE2 train, ERRI D214 bridge $L = 15$ m ($f_0 = 5$ Hz), $\zeta = 2\%$.Comparison between LIR signature method and dynamic moving load analysis.

## 2.4 Models with vehicle-structure interaction

The above models for dynamic analysis consider the traffic actions as moving loads of fixed values, whereas in reality they provide from vehicles which have their own dynamics and will not be constant. More realistic models consider coupled vehicle-bridge dynamic models including the interaction between both subsystems. In general, the consideration of interaction with vehicles will allow part of the energy of vibration of the bridge to be transferred to the vehicles, and consequently will predict lower vibrations on the bridge.

Vehicle subsystems may be generally considered as rigid bodies, with masses for wheelsets $M_w$, bogies $M_b$ and Vehicle box $M$, and concentrated springs and dampers, as shown in figure 12. Models for vertical dynamics may include only vertical translation degrees of freedom and pitch rotations for vehicle body or bogies. Complete 3D problems include all the rotations and should be handled with general multibody models, either linear or nonlinear, as described e.g. in chapter 6 or 7 of this book.

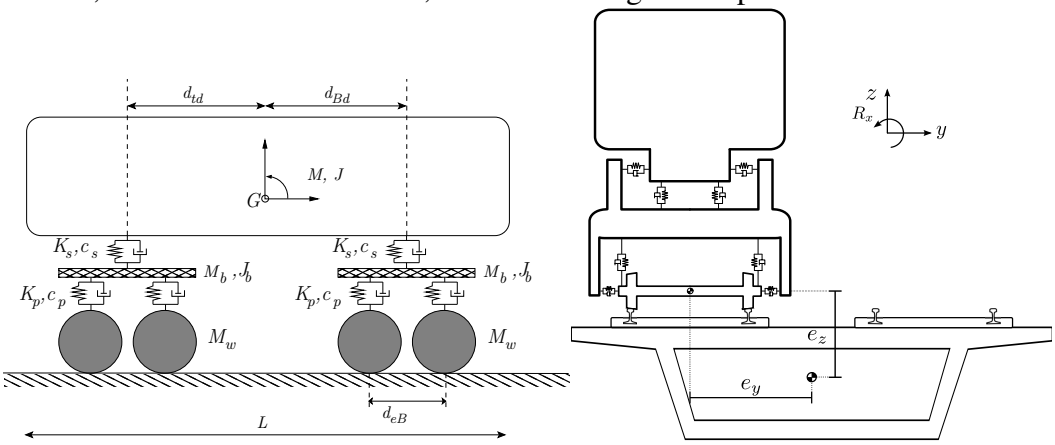


Figure 12: Models for vehicle-bridge interaction

### 2.4.1 Simplified Interaction Model

Often full vehicle-bridge interaction models are not necessary, as some parts of the vehicle will not interact with the bridge, depending on the frequencies of vibration. Bodies with frequencies which are very low with respect to the bridge will not be excited by the bridge motion and behave as constant moving loads. Bodies with frequencies which are much higher will behave as added masses.

For railway passenger vehicles under vertical motion one can identify three main frequencies: 1) vibration of wheelsets considering Hertzian contact with the rails, of the order of 100 Hz; 2) vibration of bogies on the primary suspension, of the order of 4 Hz; 3) vibration of the vehicle box, of the order of 1 Hz. In practice, the types of bridges which show greater dynamic vibrations have fundamental frequencies of the order of 3 to 7 Hz, hence the interaction will provide mainly from bogie masses and primary suspensions. Wheelset masses behave (from the point of view of bridge dynamics) as rigidly attached to rails, and vehicle box masses as moving loads of fixed value.

For such cases a simplified interaction model is convenient (figure 13): the bridge will be modelled by modal analysis with $i = 1..n$ modes, the train with $j = 1..k$ interaction elements (one per wheelset, suspended mass + moving load).

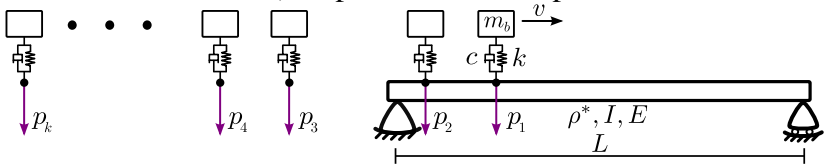


Figure 13: Simplified models for vehicle-bridge interaction

Under these assumptions, the equations for each mode of vibration ($\phi_i = 1 \ldots n$, with amplitudes $y_i$) are (details in Domínguez Barbero, 2001):

$$M_i\, \ddot{y}_i + C_i\, \dot{y}_i + K_i\, y_i = \sum_{j=1}^{k} \left\langle \phi_i \left( d^j_{\text{rel}} \right) \right\rangle \left( p^j + m^j_b\, \ddot{z}^j \right), \tag{13}$$

and for each interaction element ($z_j = 1 \ldots k$):

$$m^j_b \ddot{z}^j + k^j \left[ z^j - \sum_{i=1}^{n} y_i \; < \phi_i(d^j_{\text{rel}}) > \right]$$

$$+ c^j \left[ \dot{z}^j - \sum_{i=1}^{n} \dot{y}_i < \phi_i(d^j_{\text{rel}}) > - \sum_{i=1}^{n} y_i \; v < \phi'_i(d^j_{\text{rel}}) > \right] = 0 \tag{14}$$

These equations are simple to implement and represent only a minor extension to the moving load modal analysis equations (9), with very small computational cost.

As a representative example we show in figure 14 the results with simplified interaction models as compared to the moving load models. The case corresponds to a Talgo HS train at a high but non-resonant velocity (360 km/h) on the $L = 15$ m bridge previously described (ERRI, 1998). Quasistatic results are also shown, allowing to identify in each case the dynamic contributions to response. As expected, the

interaction models predict a moderately lower vibration of the bridge, providing more realistic results. Additionally, we show the case for a resonant velocity in figure 15. For resonance, the reduction in bridge response is more significant. However, the resonant response will still be very large and unacceptable, especially for accelerations.

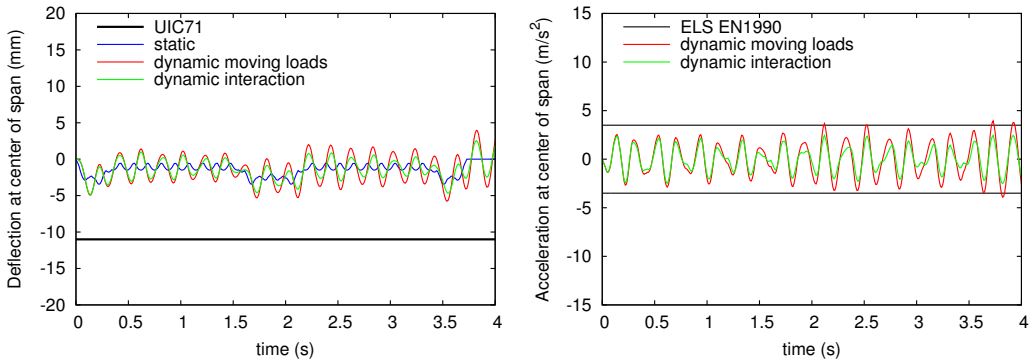


Figure 14: Talgo HS train at 360 km/h (non-resonant velocity) for $L = 15$ m ERRI D214 (ERRI, 1998), damping $\zeta = 0.01$, with interaction and moving loads.

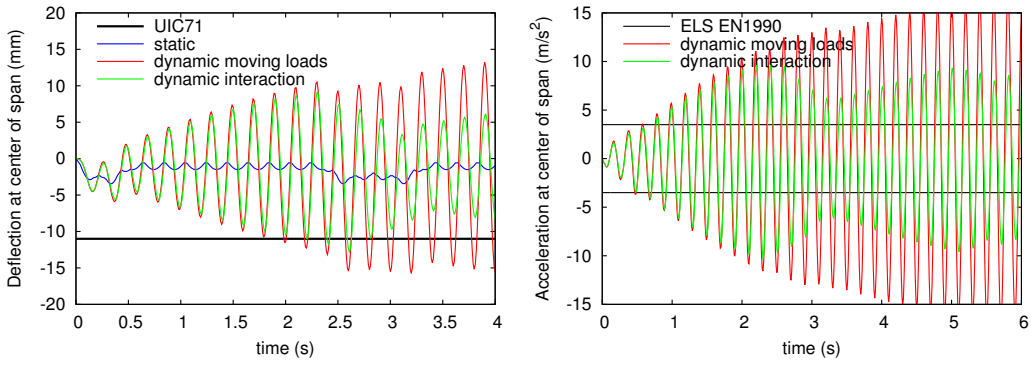


Figure 15: Talgo HS train at 236.5 km/h (resonant velocity) for $L = 15$ m ERRI D214, damping $\zeta = 0.01$, with interaction

# 3 Design issues and Applications

## 3.1 Span of the bridge

It is known that dynamic effects are of greater relevance for short or medium span bridges. There are several causes behind this behavior; in our view the main reason is the relation of the bridge span with the length of the vehicles. If the bridge span is shorter than the vehicle length, axles (or bogies) will act one at a time on the bridge, and produce resonant response for an appropriate frequency of excitation corresponding to a critical velocity. On the contrary, for bridge spans larger than vehicles, several axles will be acting simultaneously at different points of the bridge, often counteracting their respective actions, and thus reducing the resonant effects. Also, the lower mass in short bridges will produce greater accelerations.

A basic but representative application example has been analyzed, considering bridges of spans $L = 20,\ 30,\ 40$ m from the ERRI D214 catalogue (ERRI, 1998). The

analyses have been performed both with moving loads and with vehicle-bridge interaction, consisting of a velocity sweep from 120 to 420 km/h to obtain the envelope of maxima in terms of velocity, see figure 16. The $L = 20$ m bridge shows a pronounced resonant peak at near 380 km/h, and the interaction model obtains some reductions at this resonant peak; the $L = 30$ m bridge shows a less prominent resonance around 280 km/h, with smaller reduction obtained from vehicle interaction; finally, the $L = 30$ m bridge shows virtually no resonance within the velocity range considered and a very moderate dynamic response which increases slightly with speed. Virtually no influence of interaction is seen for this case.

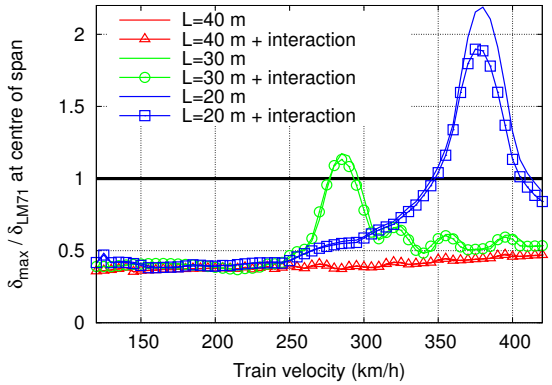


Figure 16: Normalised envelope of maximum displacements for ICE2 high-speed train between 120 and 420 km/h on simply supported bridges of different spans ($L$=20 m, $f_0$=4 Hz, r=20 t/m, $d_{LM71}$=11.79 mm, $L$=30 m, $f_0$=3 Hz, r=25 t/m, $d_{LM71}$=15.07 mm and $L$=40 m, $f_0$=3 Hz, r=30 t/m, $d_{LM71}$=11.81 mm). Dashed lines represent analysis with moving loads, solid lines with symbols models with interaction. Damping is z=2% in all cases.

## 3.2 Mass and stiffness of bridges

In order to verify the basic design options for bridges in relation to dynamic response we develop some simple analyses, which show the influence of variations in mass and stiffness. These options may be relevant for the design of bridges to reduce dynamic effects.

We consider as base case the bridge from ERRI D214 catalogue (ERRI, 1998) of $L = 20$ m, $\overline{m} = 20$ t/m, bending stiffness $EI = 20750590$ kN·m$^2$, fundamental frequency 4 Hz with damping $\zeta$ = 1%. The bridge is subject to ICE2 trains with speeds from 120 to 420 km/h. Variations in mass or stiffness influence the fundamental frequency $f_0$ as it is proportional to $\sqrt{EI/\overline{m}}$ . Furthermore, the first critical velocity is also shifted, as the expression is $v_k = D_k f_0$ for a given characteristic axle distance $D_k$.

### 3.2.1 Increase mass of bridge

Figure 17 shows the result of increasing the mass per unit length $\overline{m}$ to 25 and 30 t/m, keeping stiffness constant. The following effects are seen:

1. Frequency $f_0$ and critical speed $v_{\text{crit}}$ decrease with $\sqrt{\overline{m}}$
2. Maximum displacements at resonance are unchanged
3. Maximum accelerations at resonance decrease according to $m$.

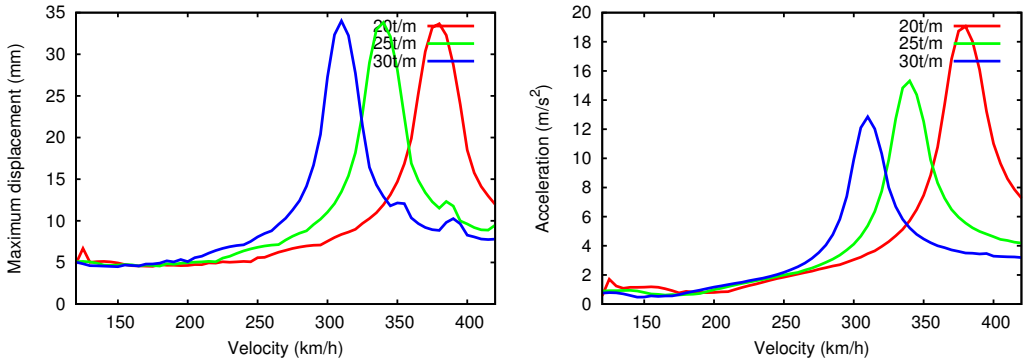


Figure 17: variation of mass of bridge – effect on displacements and accelerations.

### 3.2.2 Increase stiffness of bridge

In this case the bending stiffness $EI$ is increased from the base value by factors 1.25 and 1.5, keeping mass $\overline{m}$ constant. The fundamental frequencies obtained are respectively 4, 4.472 and 4.899 Hz. Results are shown in figure 18, showing the following effects on resonant response:

1. Frequency $f_0$ and critical speed $v_{\text{crit}}$ increase according to $\sqrt{EI}$. The increase in critical velocity has the effect of expelling the resonant peaks from the range of design velocities.
2. Maximum displacements at resonance decrease according to $1/EI$.
3. Maximum accelerations at resonance are unchanged.

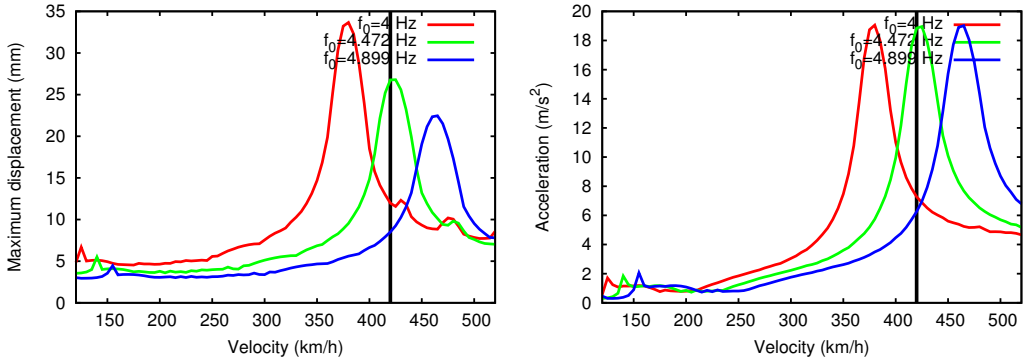


Figure 18: Variation of stiffness of bridge – effect on displacements and accelerations. The vertical black line defines the limit for the design speed, 420 km/h.

### 3.2.3 Simultaneous increase of mass and stiffness

Finally a simultaneous variation of mass and stiffness is performed, with proportions 1.25 and 1.50. The frequency is unchanged at $f_0 = 4$ Hz. Results are shown in figure 19, with the following effects on resonant response:

1. Frequency $f_0$ and critical speed $v_{\text{crit}}$ are unchanged
2. Maximum displacements at resonance decrease
3. Maximum accelerations at resonance decrease

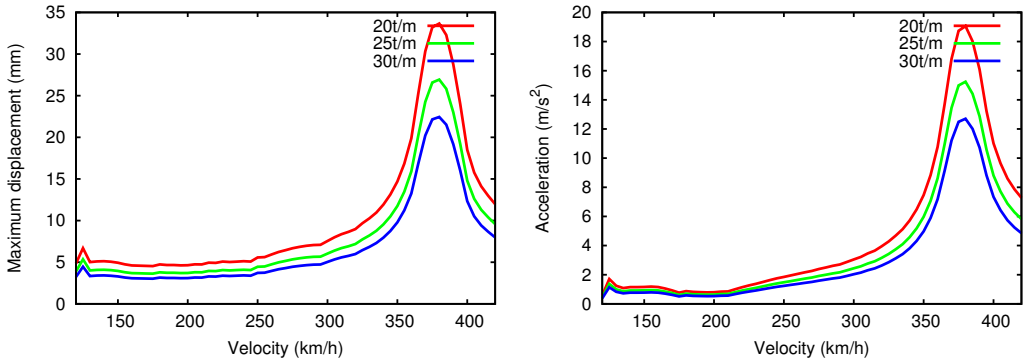


Figure 19: variation of mass and stiffness of bridge – effect on displacements and accelerations.

## 3.3 High-speed trains and dynamic load models

Several distinct types of HS trains exist in Europe, having been classified into three families (CEN, 2003): conventional (independent coaches with two bogies), articulated (coaches sharing bogies) and regular (coaches articulated on single wheelsets without bogies). In order to enable interoperability of trans-European HS lines it is necessary to consider all possible circulation speeds and all possible current and foreseeable trains. If such trains were to be checked individually this would be a difficult task.

A useful tool for ensuring interoperability is the envelope of dynamic signatures of real HS trains in Europe according to equation ($12_3$), shown in figure 20a. A fictitious family of trains has been designed to provide an envelope covering the real HS trains (EN1991-2, CEN, 2003; TSI for HS, ERA, 2006). This is called *High Speed Load Model (HSLM)* and includes a family of 10 reference trains. The envelope of HSLM is plotted in figure 20b and shows how it covers the envelope of existing HS trains.(TSI HS, ERA, 2006; EN1991-2, CEN, 2003)

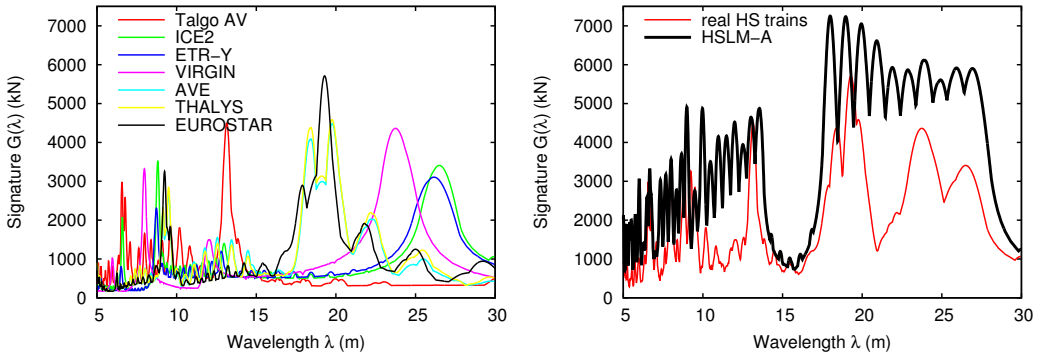


Figure 20: Signature envelopes for real HS trains and HSLM envelope.

## 3.4 Continuous bridges

Following we show in a representative example the difference in dynamic behavior of continuous deck bridges with respect to simply supported spans. The "Arroyo del Salado" Viaduct (Sanz & Goicolea, 2005) in the Córdoba-Málaga HS line has been employed for this purpose, in which the proposed solution is a continuous deck with 30 spans of 30 m each, with concrete in-situ box section, see figure 21.

For the continuous deck several modes, not just the fundamental one, participate significantly in the structural vibration. In this case 10 modes appear under 30 Hz. These modes involve deformation of the complete structure, not being limited to a single span. The six main modes are shown in figure 21, with frequencies between 4.43 Hz and 17.0 Hz. Loads from train axles will act in these modes generally not under the same phase, as a result the action of some axles will counteract the action of others. For the simply supported case the first 3 modes are for 4.43, 17.0 and 24.5 Hz. The dynamic results for accelerations are shown in figure 22, considering the 10 HSLM reference trains. For the simply supported spans (left subfigure) acceleration values are obtained clearly above the admissible limit ($3.5\ \mathrm{m/s^2}$), for the higher speeds. On the contrary, for the continuous deck (right subfigure) lower accelerations are obtained, specially for the resonant high speeds.

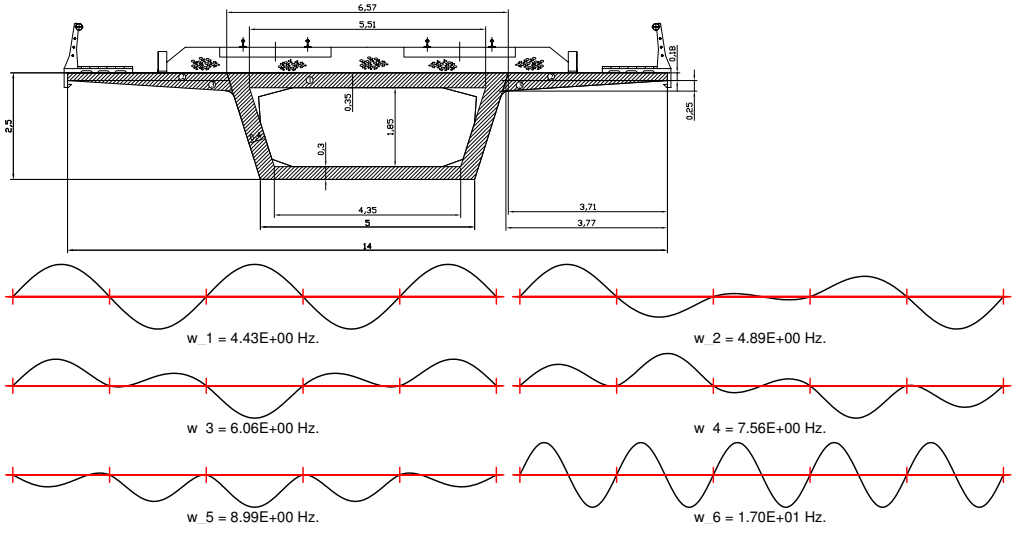

Figure 21: Continuous viaduct section for “Arroyo del Salado” and 6 first modal shapes

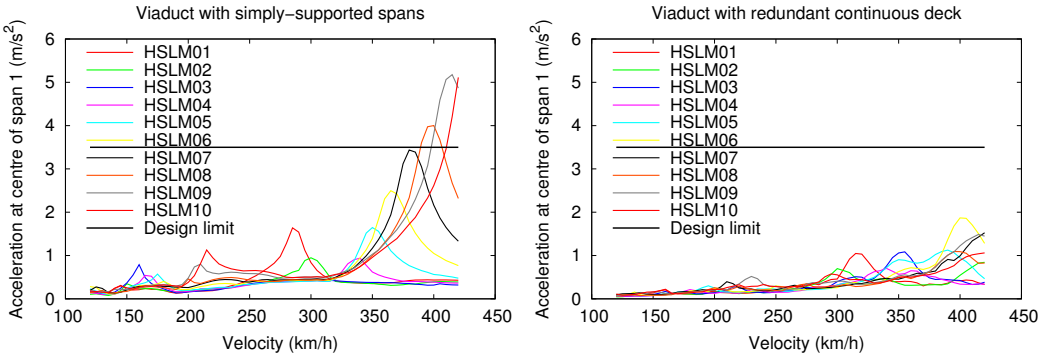


Figure 22: Acceleration envelopes for velocity sweeps. Left subfigure corresponds to simply-supported solution, right subfigure to continuous deck solution; black line defines design limit of $3.5\ \mathrm{m/s^2}$.

# 4 Conclusion

In this chapter, a critical review of methods for evaluating dynamic effects on high-speed railway bridges is performed, discussing the features and design issues. The following remarks are summarized as conclusion.

1. The analytical solution to the moving load problem allows an understanding of the maximum value of this effect and its limitations, as well as the parameters influencing dynamic response. The results are compared to the impact factors included in engineering codes for conventional rail speeds.

2. Methods for dynamic analysis based on moving loads provide the main tool at the design stages. They yield slightly conservative evaluations, which are accurate enough for most practical situations. An important issue to consider is the number of modes to employ in the computations if a modal analysis is carried out.

3. The dynamic signature methods may be an option for quick appraisal of dynamic effects and identification of critical resonant speeds. They also provide a basis for establishing dynamic load models such as HSLM (CEN, 2003; ERA, 2006).

4. Models with coupled vehicle-bridge interaction provide a more refined and less conservative evaluation, which may be of interest in special cases or for research. For short or medium span bridges simplified interaction models are advisable.

5. Two basic issues are reviewed which affect adversely the dynamic response of bridges: the short span lengths (as opposed to spans clearly longer than vehicle lengths), and the simply supported bridges (as opposed to continuous deck bridges).

6. The influence of mass and stiffness of the bridge is discussed, as their variation provides simple options for adjusting the dynamic design.

## Acknowledgements

The authors are grateful for support from Ministerio de Fomento of Spanish Government in the project *Revisión de la instrucción de acciones a considerar en el proyecto de puentes de ferrocarril* (A-VENC-E-129); from Ministerio de Ciencia e Innovación of Spanish Government in the projects *Viaductos Ferroviarios Inteligentes "VIADINTEL"* ( PSS-370000-2009-52)*, Integración de la monitorización de viaductos Ferroviarios en el Sistema de Gestión y Mantenimiento de Infraestructuras "VIADINTEGRA"* (IPT-370000-2010-012). The authors acknowledge also the support from the Technical University of Madrid, Spain

## 4.1 References

1. Clough RW, Penzien J (1993). Dynamics of Structures. New York: McGraw-Hill Inc.

2. CEN - European Committee for Standardization, 1995: ENV 1991-3. Eurocode 1, part 3: Design basis and actions on structures; traffic loads on bridges. European Union.

3. CEN - European Committee for Standardization, 2003: EN1991-2: Eurocode 1: Actions on structures - Part 2: Traffic loads on bridges. European Union.

4. CEN - European Committee for Standardization, 2005: EN1990-A1 Eurocode 0 – Basis of Structural Design, Amendment A1: Annex A2, Application for bridges. European Union.

5. Chopra AK, 2007. Dynamics of Structures: Theory and Applications to Earthquake Engineering. Prentice Hall, University of California, Berkeley (3rd edition).

6. Domínguez Barbero, J, 2001. "Dinámica de puentes de ferrocarril para alta velocidad: métodos de cálculo y estudio de la resonancia". PhD thesis (in Spanish), Technical University of Madrid. Available online http://oa.upm.es/1311/

7. ERA – European Railway Agency, 2006. "Draft Technical Specification for Interoperability of the Trans-European High-Speed Rail System, Infrastructure subsystem".

8. ERRI – European Railway research Institute, 1995. ERRI committee D181 final report: "Lateral Forces on Railway Bridges". Utrecht, The Netherlands.

9. ERRI - European Railway Research Institute, 1998. ERRI committee D214 final report: "Design of Railway Bridges for Speed up to 350 km/h; Dynamic loading effects including resonance". Utrecht, The Netherlands.

10. Goicolea, J, Antolin, P. 2011. Dynamic effects of railway traffic due to lateral motion in long viaducts with high piers. COMPDYN 2011, Corfu, Greece.

11. Goicolea, JM and gabaldón, F (2008). "Research related to vibrations from high-speed railway traffic", in *Noise and Vibration on High-Speed Railways*. Faculty of Engineering of University of Porto, Portugal; FEUP Ediçoes.

12. Lewis PR & Reynolds K. (2002) Forensic Engineering: A Reappraisal of the Tay Bridge Disaster, reinvestigating the Tay Bridge disaster of 1879, Interdisciplinary Science Reviews, Vol 27, no 4.

13. Lewis, PR (2007). Disaster on the Dee: Robert Stephenson's Nemesis of 1847, Tempus Publishing.

14. Martin T. J & MacLeod I. A. The Tay rail bridge disaster revisited, Proc. Instn Civ. Engrs, 2004 ,157, 187-192

15. Ministerio de Fomento, 2007. Instrucción de acciones a considerar en puentes de ferrocarril (IAPF). Gobierno de España.

16. Nasarre, J. 2009. Serviceability limit states in relation to the track in railway bridges. In R. Calçada et al (eds), *Bridges for High-Speed Railways*: 211-220. London: Taylor & Francis.

17. Sanz, B and Goicolea JM, 2005. Project for the viaduct for high-speed railway line on "Arroyo del Salado". Final diploma project, School of Civil Engineering, Technical University of Madrid (2005).

18. Stokes, G.G., 1849. Discussion of a differential equation related to the breaking of railway bridges. Transaction of the Cambridge Philosophical Society 8, 707–735.

19. Tartary JP and Jobert N, 2000. "Recherche du train universel pour calculs dynamics". Report for ERRI D214 committee, A.V.L.S. (may 2000).

20. Timoshenko, S.P. "Vibration problems in engineering". Van Nostrand (1928).

21. UIC - Union Internationale des Chemins de Fer, 1979. "Fiche UIC 776-1R: Charges a prendre en consideration dans le calcul des ponts-rails". 3 ed, jul 1979.

22. UIC - Union Internationale des Chemins de Fer, 2006. "Fiche UIC 776-1R: Charges a prendre en consideration dans le calcul des ponts-rails". 5 ed, aug 2006.

23. Willis, R., 1849. Appendix to the Report of the Commissioners Appointed to Inquire into the Application of Iron to Railway Structures. H.M. Stationary Office, London, UK.



View publication stats